Journal of Environment and Earth Science
ISSN 2224-3216 (Paper) ISSN 2225-0948 (Online)
Vol.12, No.9, 2022

Temporal Rainfall Anomaly and Its Association with Crop Yield: In the Case of Afar Region, Ethiopia

Tadele Badebo
National Meteorological Institute of Ethiopia
P.O.box 1090, Addis Abab, Ethiopia
E-mail of the corresponding author: tadele_bdebo@yahoo.com

Abstract
Ethiopian economy is predominantly agrarian and the majority of the population in the country engaged in agricultural activities which is considerably affected by rainfall variability. The majority of the nation's crops are rain-fed, making them particularly vulnerable to the fluctuation that can cause severe food insecurity, which can result in famine and poverty over the whole nation. The impact of rainfall variability was very serious in the pastoral areas that are largely inhabited by the pastoralist whose livelihood depend primarily on livestock farming. For this study, rainfall data were taken from Ethiopian Meteorology Institute (EMI) for 1981-2020 period and yield data were taken from Central Statistical Agency (CSA) of Ethiopia for 1994-2019 period. This study was briefly evaluated rainfall variability and its impact on yield and computed Rainfall Anomaly Index (RAI) for Kiremt cropping season in a pastoral area of Afar region, Ethiopia. Regression analysis for the Kiremt cropping season based on observed rainfall dataset was used in the study to further analyze the relationship between rainfall variability and yield. The temporal analysis of RAI clearly indicated that there were more dry years than wet years with varies magnitude. The year of 1984 and 2009 were found extremely dry with magnitude of -4.95 and -4.13, respectively whereas 1987, 2015, 2002, 2004 and 1997 were identified as very dry with magnitude of -3.92, -3.39, -3.16, -2.88 and -2.41, respectively. The year of 1988 and 1998 found extremely humid with magnitude of 5.87 and 5.33 whereas 2020, 1994, 2010 and 1992 were very humid with magnitude of 3.47, 3.20, 2.98 and 2.34 respectively. The outcome of the regression analysis showed a positive link between rainfall anomaly and crop production for the Kiremt cropping season, with yield increasing with a positive rainfall anomaly and rainfall anomaly accounting for 29.4% of crop yield.
Keywords: Kiremt Cropping Season, Rainfall Anomaly Index, Pastoral Area, Regression, Yield
DOI: 10.7176/JEES/12-9-03
Publication date: September 30th 2022

1 Introduction

The amount of rain that falls in a given area over the course of a year typically varies from the amount that fell in the same area the year before or after. Rainfall is typically described as normal, above normal, and below normal, respectively, according to the World Meteorological Organization (WMO). In this context, normal is defined as the average amount of rainfall during a given time period—typically 30 years or more—on an annual, monthly, or other basis (WMO, 2017).

Rainfall variability is defined by the Intergovernmental Panel on Climate Change (IPCC) as variations in rainfall frequency over or under a long-term average. Every year, at a certain time, the rainfall in an area can vary, either above or below average; this is called variability (IPCC, 2007), however, the mean does not change throughout the year. According to numerous scholars, Ethiopia's seasonal rainfall pattern can be divided into three climatological rainy seasons (Korecha & Barnston, 2007). These three separate seasons are, respectively, the dry (October to January), minor rainy (February to May), and major rainy (June to September). The Bega (October–January), Belg (February–May), and Kiremt seasons as they are known locally (June-September). According to Korecha & Barnston, (2007) the country's high agricultural output and significant water reservoirs receive 50%–80% of their yearly rainfall during the Kiremt rains between June and September (JJAS). As a result, the most severe droughts are typically caused by the JJAS rainfall failing to satisfy Ethiopia's agricultural and water resource needs (Korecha & Barnston, 2007).

The El-Nio Southern Oscillation (ENSO) events and other multiscale ocean-atmosphere interactions are primarily responsible for Ethiopia's rainfall variability. The ENSO occurrences affect the seasonal rainfall pattern widely and cause the country's annual rainfall variance (Wolde-Georgis, 1997**,** Korecha & Barnston, 2007, Kelem & Derbew, 2017). In Ethiopia, most of historical droughts and famines occurred during El-Niño years, its severity and spatial extent varied from year to year, depending on time of the year Niño emerged and its strength. For example, the major El-Niño events during Kiremt season were recorded in the year of 1987, 1991, 1997, 2002, 2004, 2006, 2009, 2014, 2015, 2018 and 2019, respectively. Very strong El-Niño was recorded in the year of 1997 with magnitude of 1.6 to 2.1 during Kiremt season and 2.2 to 2.4 in Bega season, respectively. Similarly, very strong El-Niño was recorded in the year of 2015 with magnitude of 1.5 to 2.2 in main rainy season (JJAS) and 2.4 to 2.6 in Bega season, respectively. Some drought years have coincided with

ENSO events, while others have followed it and show a remarkable association (Hu et al., 2020). More details of El-Niño are available at Oceanic Niño Index [1]. The Famine Early Warning System Network (FEWSNET) reports indicated that Ethiopia faced massive drought and food insecurity crises as a result of failed rain that have been worsened by the 2015 El-Niño. As a result, millions of people have affected and lost food, water and livelihood (FEWSNET, 2016).

Ethiopian economy is predominantly agrarian and the majority of the population in the country engaged in agricultural activities which is considerably affected by rainfall variability. Because the majority of the nation's crops are rain-fed, acute food insecurity is a risk that this important source of livelihood faces (Gezie, 2019). Food insecurity is a result of the net potential impact of rainfall unpredictability, which eventually causes poverty and famine (Kyei-mensah et al., 2019). Pastoralism dominates the way of life in the Afar Region. However, the pastoral method of production has occasionally been contested owing to persistent drought, which led to a decline in the number of animals, and pastoral households have turned to alternate livelihoods like agro-pastoralism. According to CSA, agro-pastoralism has long been practiced in Afar and accounts for around 10% of the local economy there. A sizeable majority of households in the area currently work in crop cultivation. Teff, Barley, Wheat, Maize, and Sorghum are reported to be the cereal crops most frequently planted in the area (CSA, 2021). One of the most crucial climatic factors in crop production is rainfall. Crop production is influenced by its commencement, end, amount, distribution, and inter-seasonal variability.

Study on yield- rainfall relationship showed that moisture shortage determined in yield that total growing season and critical month rainfall-yield was strong (Huang et al., 2015). The following examples show how agricultural yield and climatic variability are related (Teshome, 2017). The results showed that rainfall variability has an impact on production and greatly reduces the low yield variability by up to 60% (Potopova et al., 2016). The goal of this study is to assess temporal rainfall anomalies and their associations with yield using regression analysis and the rainfall anomaly index based on observed rainfall and yield dataset.

2 Materials and Methods

2.1 Description of study area

One of Ethiopia's ten administrative states, the Afar area (Figure 2- 1) is situated in the northeastern section of the country between 8° 51' and 14° 34' N and between 39° 47' and 42° 24' E. The region has an area of about 94,760 square Kilometers and divided into five administrative Zones namely Awsi Rasu (Administrative zone 1), Kilbet Rasu (Administrative *Zone* 2), Gabi Rasu (Administrative *Zone* 3), Fanti Rasu (Administrative *Zone* 4) and Hari Rasu (Administrative *Zone* 5) that are further subdivided in to 32 districts (Woredas), respectively. The region is topographically diverse, with elevations ranging from 125 m below sea level to 2,870 m above sea level (Wakie et al., 2014, Luizza et al., 2016).

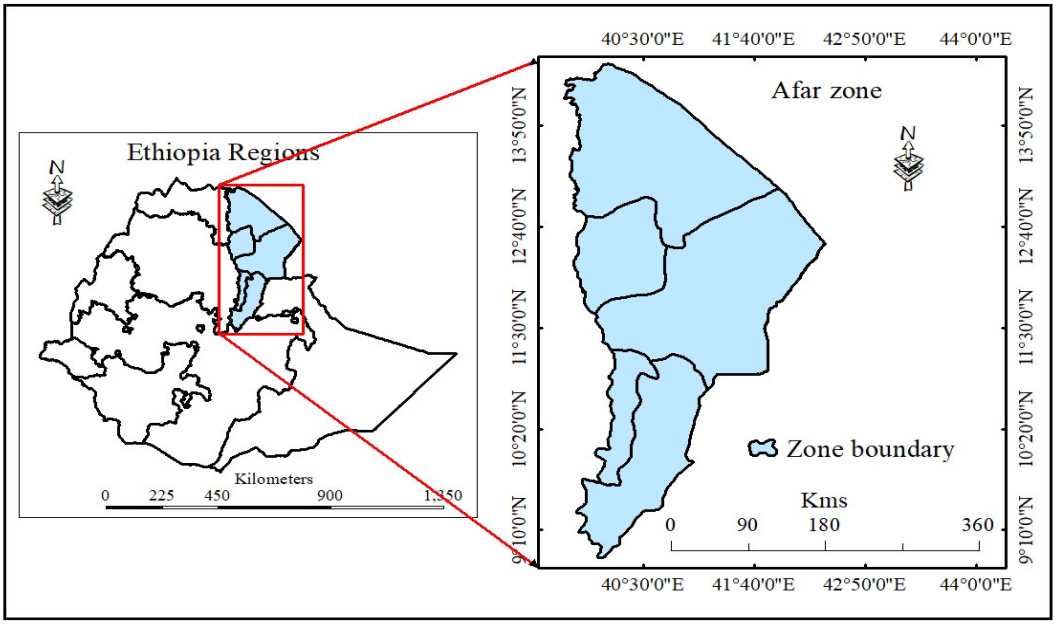

Figure 2- 1 Ethiopia regions and study area map

[1] https://origin.cpc.ncep.noaa.gov/products/analysis_monitoring/ensostuff/ONI_v5.php

2.2 Materials

The references are cited and inserted using the American Psychological Association (APA) in-text and reference list citation style, and Python 3 (version 3.9), which is downloaded from the source, is used to complete the missing data and correct bias. For correlation and regression analysis, the program SV26|IBM SPSS Statistics 26 is used, and it is accessible at[1].

2.3 Data Types and Sources

2.3.1 Station Observation

The EMI provided the daily rainfall data for 44 gauge sites used in this study for the years 1981 to 2020. There are 2% to 86% of rainfall data available. The precipitation data from Climate Hazards Group Infrared Precipitation (CHIRP) for the 1981–2020 periods is obtained and extracted for 44 stations using their respective Latitude and Longitude due to missing data in the observation dataset (Appendix 1).

2.3.2 CHIRP Precipitation Data

To complete the gaps in observation and accessible data, the CHIRP data set is employed. The CHIRP products have been described in depth in the (Funk et al., 2015). The CHIRP product is a brand-new land-only infrared (IR)-based climate precipitation dataset with high spatial resolution (0.05° 0.05°), long-term records (1981–present), and temporal resolutions of daily, monthly, and yearly (Katsanos et al., 2016, Funk et al., 2015). It is created by the University of California and the United States Geological Survey. A variety of drought monitoring and assessment projects used the CHIRP dataset(Tuo et al., 2016, Dinku et al., 2018, Wu et al., 2019, Kebede et al., 2020). Both the country level and the regional level for eastern Africa are analyzed.

2.3.3 Crop Yield data

The CSA of Ethiopia provided the crop yield data for the years 1994/1995 to 2019/20. The dataset includes a regional level of kiremt crop for the Afar region, which is typically planted during the main wet season (JJAS). The dataset includes both the volume of crop production reported by CSA in quintals (qt) for each year and the total area of cropped land for the entire Afar region in hectares (ha).

2.4 Methods

2.4.1 Rainfall Anomaly Index (SAI)

To show the intra-seasonal and annual variance of rainfall with long year mean, rainfall anomalies are displayed against time (in years). In the rainfall record, this indicator is used to identify the dry and rainy years. Calculated mathematically as:

$$RAI = 3 * \frac{(N-\dot{N})}{(\acute{M}-\dot{N})} \qquad \text{Eqn 2- 1}$$

$$RAI = -3 * \frac{(N-\dot{N})}{(\hat{u}-\dot{N})} \qquad \text{Eqn 2- 2}$$

where Eqn 2.2 for positive anomalies and Eqn 2.3 for negative anomalies, respectively.
N = current monthly/yearly rainfall, in order words, of the month/year when RAI will be generated (mm); $\dot{N}$ = monthly/yearly average rainfall of the historical series (mm); $\acute{M}$= average of the ten highest monthly/yearly precipitations of the historical series (mm); $\hat{u}$= average of the ten lowest monthly/ yearly precipitations of the historical series (mm); and positive anomalies have their values above average and negative anomalies have their values below average.

Table 1: Classification of Rainfall Anomaly Index Intensity

	RAI range	Classification
Rainfall Anomaly Index	Above 4	Extremely humid
	2 to 4	Very humid
	0 to 2	Humid
	-2 to 0	Dry
	-4 to -2	Very dry
	Below -4	Extremely dry

2.4.2 Crop Yield Reduction

In order to estimate the relationship and strength of crop yields with Rainfall Anomaly Index for the study area, crop yield data for the years 1994/1995 to 2019/2020 were obtained from the CSA of Ethiopia and climate data for 44 stations were obtained from the EMI. Crop yield and climate both contain temporal datasets, with yield representing an area production for the entire region from 1994 to 2020 and climate being a point observation from 44 sites from 1981 to 2020. We have integrated the climate data from 44 sites for the entire region and computed the Rainfall Anomaly Index for the years 1981 to 2020 in order to investigate the dry and wet seasons. Furthermore, the yield dataset only includes data for the JJAS (kiremt cropping) season from 1994/95 to 2019/20

[1] https://*www.ibm.com*/support/pages/*downloading-ibm-spss-statistics-26*

and Rainfall Anomaly Index computed from 1994 to 2020 to investigate the relationship between yield and rainfall anomaly.

In addition to climate, there are other variables that affect yield throughout time, including new management practices and technologies, which frequently result in a rising trend in the yield. The de-trended yield is used to eliminate the impact of these non-climatic elements and isolate the variance brought on by climate (Asner, 2003, Potopova et al., 2016). According to Wu et al., (2004), the residuals of the de-trended yield $Y_i^{(T)}$ can be used as an indicator of the danger of an agricultural drought. The region-wide yield lost during the Kiremt farming season is computed as follows:

$$\mathbf{Y_i^{(T)} = Y_i^0 - Y_i^{(\tau)}} \qquad \text{Eqn 2-3}$$

where Y_i^0 is the observed crop yield and $Y_i^{(\tau)}$ is the value of the de-trended yield in a distinct year. To fit the series of $Y_i^{(T)}$ we used the same log-logistic distribution probability function, which showed a very close fit to both series (Potopová et al., 2015).

The residuals of yields from detrending represent the impact of the climate on agricultural yield (Potopova et al., 2016, Wheeler, 2015, Hussain et al., 2018, Vogel et al., 2019). The series of $Y_i^{(T)}$) were standardized using the Z-score transformation in order to assess yield variability with varied means and standard deviations. In order to calculate the Standardized Residual Yield Series (SRYS),

$$\mathbf{SRYS} = \frac{Y_i^{(T)} - \mu}{\sigma} \qquad \text{Eqn 2-4}$$

where $Y_i^{(T)}$ is the yield residual, μ is the mean of the yield residuals and σ is the standard deviation of yield residuals. The various yield loss categories are defined in Table 3.4 (Thenkabail et al., 1994, Hamal et al., 2020).

Table 3.4: Yield loss classification

SRYR values	Yield loss category
-1.0< SRYR <= -0.5	Low yield loss
-1.5< SRYR <= -1	Moderate yield loss
SRYR <= -1.5	High yield loss

2.4.3 Regression

One of the most popular and straightforward methods for analyzing relationships between one dependent (y) and one independent (x) variable is regression analysis (Wagschal, 2016, Sellam & Poovammal, 2016). Regression models are generally noted as:

$$\boldsymbol{y = \alpha + \beta_1 x_1 + \varepsilon} \qquad \text{Eqn 2-5}$$

where y represents dependent variable called Crop Yield, which is the variable trying to explain, α is the constant (intercept) of the regression model, and indicates what would be dependent variable if all of the independent variables were zero, β_1 indicates the regression coefficient of independent variable x_1 called rainfall anomaly. The coefficient represents the gradient of the line and also referred to as slope. A positive β_1 coefficient indicates upward slope regression line while a negative β_1 indicates downward slope regression line (Stellefson et al., 2008, Sellam & Poovammal, 2016, Ali & Younas, 2021). The symbol $\boldsymbol{\varepsilon}$ is a random error components and signifies imprecision of regression indicating that, in actual practice the independent variables are cannot perfectly predict the change in any dependent variables (Montgomery et al., 2021).

3 Results and Discussion

3.1 Rainfall Anomaly Index

With positive numbers indicating wet or rainy years and negative values indicating dry years with varied degrees of intensity, RAI can be used to display the dry and wet years between 1981 and 2020. Figure 3-1 displays the dry and rainy periods as well as the areas where these occurrences were more severe and persistent. The 40 years that were analyzed indicated a RAI with a magnitude ranging from -0.01 to -4.96 in 21 years and a magnitude ranging from 0.09 to 5.87 in the remaining 19 years, respectively. The Kiremt cropping season in the Afar Region was extremely dry in the years 1984 (-4.95), 2009 (-4.13), 1987 (-3.92), 2015 (-3.39), and 2002 (Figure 3-1).

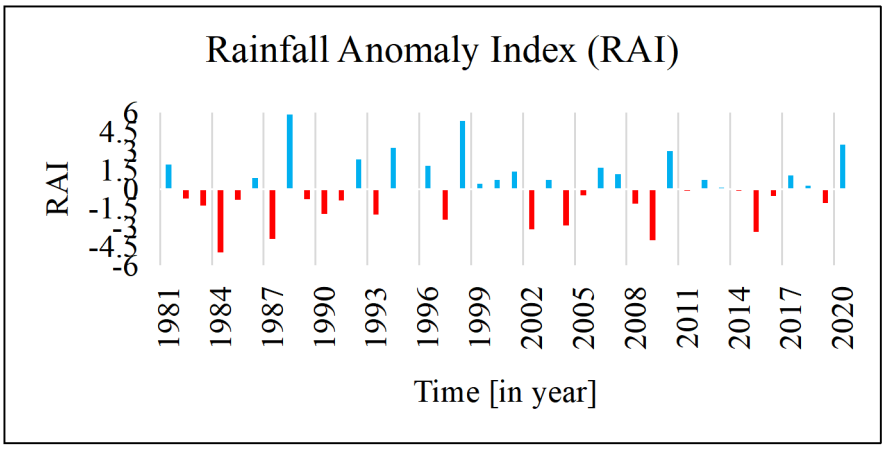

Figure 3- 1 Rainfall Anomaly Index for the Afar Region 1981-2020 period.

In Ethiopia, most of historical droughts and famines occurred during El-Niño years, its severity and spatial extent varied from year to year, depending on time of the year Niño emerged and its strength. For example, the major El-Niño events during kiremt cropping season were recorded in the year of 1987, 1991, 1997, 2002, 2004, 2006, 2009, 2014, 2015, 2018 and 2019, respectively which are coincided with dry years over Afar region (Figure 3- 1). Very strong El-Niño was recorded in the year of 1997 with magnitude of 1.6 to 2.1 during Kiremt cropping season and 2.2 to 2.4 in Bega season, respectively. Similarly, very strong El-Niño was recorded in the year of 2015 with magnitude of 1.5 to 2.2 in main rainy season (JJAS) and 2.4 to 2.6 in Bega season, respectively. The year of 1997 and 2015 were very dry years over Afar Region during Kiremt cropping season. Some drought years have coincided with ENSO events, while others have followed it and show a remarkable association (Hu et al., 2020). More details are available at Oceanic Niño Index [1]. Reports indicated that Ethiopia faced massive drought and food insecurity crises as a result of failed rain that have been worsened by the 2015 El-Niño. As a result, millions of people have affected and lost food, water and livelihood (FEWSNET, 2016). According to National Meteorological Service Agency (NMSA) report, the total rainfall of JJAS 1997 was 20% less than 1996 period and affected land preparation, sowing which adversely affected the maturation stage of the crops (Wolde-georgis & Members, 2000).

3.2 Regression Analysis Result

Scatter plot of RAI against Yield Residual showing positive relation between RAI and Yield Residual for the Kiremt cropping season with coefficient of correlation is 0.54. In Figure 3- 2 (a), the straight red line represents the regression line and (b) represents SYRS, respectively. The result of regression analysis revealed that positive correlation between RAI and crop yield anomaly for Kiremt cropping season, 29.4% of crop yield can be explained by RAI (Figure 3- 2).

The results of increasing yield losses, significant at 0.05 level in the SYRS, with high yield reduction in the year of 1997, 2002, 2015 and 2019, respectively. The other Kiremt crop yield lost were observed in the year of 1994, 1995, 1997, 1998, 1999, 2002, 2003, 2008, 2009, 2015, 2016, 2018 and 2019 (Figure 3- 2) (b), respectively. Details of regression analysis results were presented in appendix (Appendix 2).

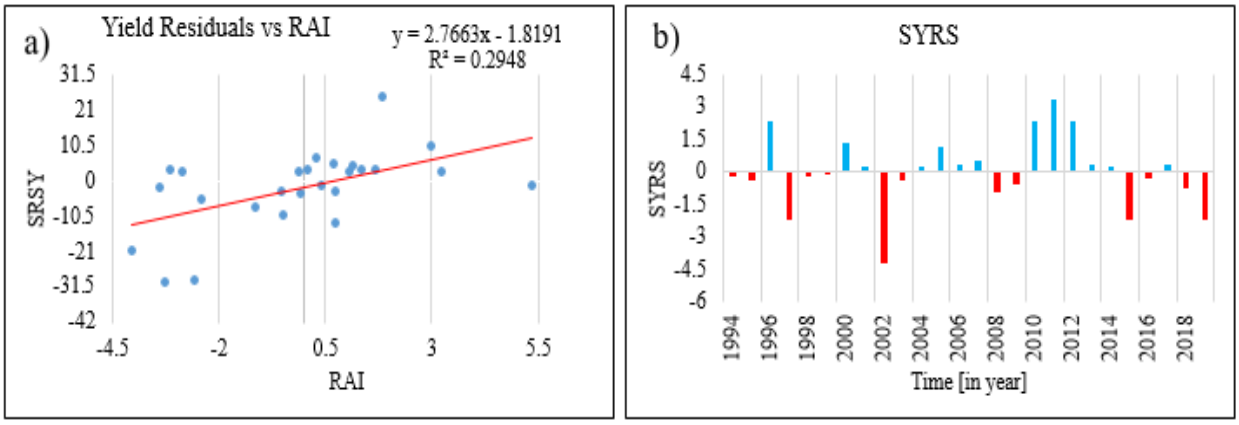

Figure 3- 2 Relationship between Rainfall Anomaly Index and Yield Residual (a) and SYRS (b).

[1] https://origin.cpc.ncep.noaa.gov/products/analysis_monitoring/ensostuff/ONI_v5.php

4 Conclusion and Recommendation

4.1 Conclusion

This study was briefly evaluated temporal Rainfall Anomaly for 1981-2020 period using RAI and its impact on crop production using crop yield for Kiremt cropping season over Afar Region by means of yield separation method and standardized residual series during 1994-2019 period. Among 40 years, 21 years were identified as dry with varies magnitude and this should be considered as 52.5%. The finding clearly indicated that 1984 (-4.95), 2009 (-4.13), 1987 (-3.92), 2015 (-3.39), 2002 (-3.16), 2004 (-2.88) and 1997 (-2.41) were extremely and very dry years, respectively over the Region. The dry years were closely related to the ENSO phenomenon which were significantly affected Kiremt rainfall pattern. The analyzed Rainfall Anomaly Index showed that the humid period occurred with the maximum precipitation for the year 1988, 1998, 2020 and 1994 respectively. The results also clearly revealed that extremely and very wet years were 1988 (5.87), 1998 (5.33), 2020 (3.47) and 1994 (3.20), 2010 (2.98) and 1992 (2.34), respectively. However, the results of Rainfall Anomaly Index showed that more dry years were identified when comparing to wet years, 52.5% of the analyzed years were considered as dry years.

The result of regression analysis revealed that positive correlation between rainfall anomaly and crop yield for Kiremt cropping season, yield increased with positive rainfall anomaly. Impact of dry spell on crop yield clearly visible over the study area, 10.9% of crop yield can be explained by rainfall anomaly. The Kiremt crop yield lost were observed in the year of 1999, 1998, 2015, 1997, 2017, 1996, 2016, 1995, 2010, 2009, 1994 and 2008, respectively.

4.2 Recommendation

More people are seriously impacted by rainfall anomalies than by any other natural disaster, and this has serious negative effects on the economy, society, and environment. The following suggestions are given in order to ensure that the benefits of this study are realized and suitable actions are made by various stakeholders. To reverse the socio-economic and ecological effects of the rainfall anomaly, the creation of a workable pastoral strategy for climate variability impact requires strong and urgent links with other development and research players. It is advantageous and so advised to incorporate the study's findings when developing development strategies for the region's early warning and planning systems based on ENSO. This research should be expanded to include other drought- and flood-prone regions of the nation and the effects of the climate.

5 Reference

CSA. (2021). *the Federal Democratic Republic of Ethiopia Central Statistical Agency Report on Area , Production and Farm Management Practice of Belg Season Crops for Private Peasant Holdings*. *V*, 25.

Dinku, T., Funk, C., Peterson, P., Maidment, R., Tadesse, T., Gadain, H., & Ceccato, P. (2018). Validation of the CHIRPS satellite rainfall estimates over eastern Africa. *Quarterly Journal of the Royal Meteorological Society*, *144*(August), 292–312. https://doi.org/10.1002/qj.3244

FEWSNET. (2016). Illustrating the extent and severity of the 2015 - 16 drought. *Famine Early Warning Systems Network/USAID Southern Africa Special Report*, 1–8.

Funk, C., Peterson, P., Landsfeld, M., Pedreros, D., Verdin, J., Shukla, S., Husak, G., Rowland, J., Harrison, L., Hoell, A., & Michaelsen, J. (2015). The climate hazards infrared precipitation with stations - A new environmental record for monitoring extremes. *Scientific Data*, *2*(December). https://doi.org/10.1038/sdata.2015.66

Gezie, M. (2019). Farmer's response to climate change and variability in Ethiopia: A review. *Cogent Food and Agriculture*, *5*(1). https://doi.org/10.1080/23311932.2019.1613770

Hamal, K., Sharma, S., Khadka, N., Haile, G. G., Joshi, B. B., Xu, T., & Dawadi, B. (2020). Assessment of drought impacts on crop yields across Nepal during 1987–2017. *Meteorological Applications*, *27*(5), 1–18. https://doi.org/10.1002/met.1950

Hu, Z., McPhaden, M. J., Kumar, A., Yu, J., & Johnson, N. C. (2020). Uncoupled El Niño warming. *Geophysical Research Letters*, *47*(7), e2020GL087621.

Huang, C., Duiker, S. W., Deng, L., Fang, C., & Zeng, W. (2015). *Influence of Precipitation on Maize Yield in the Eastern United States*. 5996–6010. https://doi.org/10.3390/su7055996

Kebede, A., Raju, U. J. P., Korecha, D., & Nigussie, M. (2020). Developing new drought indices with and without climate signal information over the Upper Blue Nile. *Modeling Earth Systems and Environment*, *6*(1), 151–161. https://doi.org/10.1007/s40808-019-00667-y

Kelem, G., & Derbew, A. (2017). The Frequency of El-Niño and Ethiopian Drought. *National Meterology Agency*, *February*, 2–3. https://doi.org/10.13140/RG.2.2.25826.73922

Korecha, D., & Barnston, A. G. (2007a). Predictability of June-September rainfall in Ethiopia. *Monthly Weather Review*, *135*(2), 628–650. https://doi.org/10.1175/MWR3304.1

Korecha, D., & Barnston, A. G. (2007b). Predictability of june–september rainfall in Ethiopia. *Monthly Weather*

Review, *135*(2), 628–650.

Kyei-mensah, C., Kyerematen, R., & Adu-acheampong, S. (2019). *Impact of Rainfall Variability on Crop Production within the Worobong Ecological Area of Fanteakwa District , Ghana*. *2019*.

Lobell, D. B., & Asner, G. P. (2003). Climate and Management in U . S . Agricultural Yields. *Science*, *299*(February), 1032. https://doi.org/10.1126/science.1078475

Luizza, M. W., Wakie, T., Evangelista, P. H., & Jarnevich, C. S. (2016). Integrating local pastoral knowledge, participatory mapping, and species distribution modeling for risk assessment of invasive rubber vine (Cryptostegia grandiflora) in Ethiopia's Afar region. *Ecology and Society*, *21*(1). https://doi.org/10.5751/ES-07988-210122

Montgomery, D. C., Peck, E. A., & Vining, G. G. (2021). *Introduction to linear regression analysis*. John Wiley & Sons.

Murphy, R. (2020). Disasters. *Essential Concepts of Global Environmental Governance*, 66–68. https://doi.org/10.7591/9781501701498-008

Potopova, V., Boroneanţ, C., Boincean, B., & Soukup, J. (2016). Impact of agricultural drought on main crop yields in the Republic of Moldova. *International Journal of Climatology*, *36*(4), 2063–2082.

Potopová, V., Štěpánek, P., Možný, M., Türkott, L., & Soukup, J. (2015). Performance of the standardised precipitation evapotranspiration index at various lags for agricultural drought risk assessment in the Czech Republic. *Agricultural and Forest Meteorology*, *202*, 26–38.

Sellam, V., & Poovammal, E. (2016). Prediction of crop yield using regression analysis. *Indian Journal of Science and Technology*, *9*(38). https://doi.org/10.17485/ijst/2016/v9i38/91714

Teshome, M. (2017). *Perceived Impact of Climate Change on Crop Yield Trend in Denbia Woreda of Amhara Region , Northwest Ethiopia*. *2*(7). https://doi.org/10.15406/mojes.2017.02.00047

Wagschal, U. (2016). Regression analysis. In *Handbook of Research Methods and Applications in Political Science* (Issue March 2014). https://doi.org/10.7748/nr1996.10.4.1.318.c6066

WMO. (2017). Guidelines on the Calculation of Climate Normals. *WMO-No. 1203*, *1203*, 29. https://library.wmo.int/doc_num.php?explnum_id=4166

Wolde-georgis, T., & Members, T. (2000). *The Case of Ethiopia*. 1–73.

Wu, H., Hubbard, K. G., & Wilhite, D. A. (2004). An agricultural drought risk-assessment model for corn and soybeans. *International Journal of Climatology: A Journal of the Royal Meteorological Society*, *24*(6), 723–741.

Appendix

Appendix 1 Stations and their geographical location

No	Station name	Code	Lat	Lon	Elv
1	Abala	ABL01	13.34	39.76	1441
2	Adaitu	ADT02	11.11	40.78	507
3	Afambo	AFM03	11.51	41.567	342
4	Afdera	AFD04	13.2	40.86	104
5	Argoba	ARG05	9.55	39.88	1331
6	Asara	ASR06	10.39	40.14	978
7	Assaita	AST07	11.53	41.52	372
8	Awaramelka	AWR08	9.16	39.98	960
9	Awasharba	AWA09	9.14	40.15	826
10	Awashsebat	AWS10	8.98	40.15	923
11	Awashsheleko	AWK11	9.33	40.25	737
12	Awura	AUR12	12.05	40.06	875
13	Berhaile	BRH13	13.86	40.01	679
14	Bidu	BDU14	12.81	40.97	31
15	Bure	BRE15	12.35	42.16	512
16	Chifra	CFR16	11.61	40.02	926
17	Dalifagi	DLG17	10.62	40.32	650
18	Dawe	DAW18	10.81	40.18	992
19	Ditchoto	DHT19	11.54	41.34	463
20	Dobi	DBI20	11.52	41.42	463
21	Dubti	DBT21	11.723	41.01	376
22	Elidar	ELD22	12.067	41.55	442
23	Elwiha	ELW23	11.25	40.38	670
24	Endifo	END24	10.52	40.75	856

No	Station name	Code	Lat	Lon	Elv
25	Erebti	ERB25	13.26	40	872
26	Ewa	EWA26	11.82	39.92	1071
27	Galafi	GLF27	11.73	41.83	144
28	Gedamaitu	GDM28	9.73	40.45	793
29	Gerjele	GRJ29	11.39	41.49	370
30	Gewane	GWN30	10.15	40.633	568
31	Harsis	HRS31	11.48	40.52	456
32	Kasagita	KSG32	11.08	40.2	888
33	Kuneba	KNB33	13.98	39.87	1179
34	Logia	LGA34	11.65	41	393
35	Manda	MND35	12.24	42.11	657
36	Megale	MGL36	12.82	39.92	1150
37	Melkasedi	MLK37	9.23	40.17	749
38	Mille	MLL38	11.42	40.77	487
39	Semera	SMR39	11.74	41	434
40	Serdo	SRD40	11.95	41.31	480
41	Slisa	SLS41	12.4	41.183	474
42	Telalak	TLK42	10.91	40.2	871

Appendix 2 Simple linear regression between Rainfall Anomaly Index and Yield

Regression Statistics	
Multiple R	0.54299472
R Square	0.29484327
Adjusted R Square	0.26546174
Standard Error	9.9721983
Observations	26

ANOVA					
	df	SS	MS	F	Significance F
Regression	1	997.927	997.927	10.035	0.004
Residual	24	2386.674	99.445		
Total	25	3384.6			

	Coefficients	Standard Error	t Stat	P-value	Lower 95%	Upper 95%	Lower 95.0%	Upper 95.0%
Intercept	-1.819	1.958	-0.929	0.362	-5.860	2.221	-5.860	2.221
X Variable 1	2.766	0.873	3.168	0.004	0.964	4.569	0.964	4.569